



# Impact of carbonization parameters on anatomic aspects and near-infrared spectra of three species from Mozambique

Silvana Nisgoski<sup>1</sup> · Helena Cristina Vieira<sup>2</sup> · Thaís Alves Pereira Gonçalves<sup>3</sup> · Claudio Manuel Afonso<sup>4</sup> · Graciela Inés Bolzon de Muñiz<sup>1</sup>

Received: 13 March 2019 / Published online: 2 November 2019  
© Springer-Verlag GmbH Germany, part of Springer Nature 2019

## Abstract

This study characterizes charcoal from *Androstachys johnsonii* (Picrodendraceae), *Bobgunnia madagascariensis* (Fabaceae) and *Sterculia quinqueloba* (Malvaceae), made by different carbonization processes, based on wood anatomy and NIR spectroscopy to verify the impact of the parameters and contribute to a database for charcoal identification and control. In the three species analyzed, changes in anatomical characteristics after carbonization were different and formed groups regarding charcoal programs as a result of anatomical and chemical characteristics. In vessel and ray dimensions and frequency, no linear relation to total time or final carbonization temperature was observed, although there were some interactions between species and program conditions. In the near-infrared spectra, the region from 4000 to 5000  $\text{cm}^{-1}$  showed more distinction between the charcoal programs. There was a separation of samples carbonized with lower intensity (400 °C and 40 min), denoting minor chemical degradation of species, from samples submitted to other programs with a final temperature of 450 °C and total time between 2 and 6 h. Near-infrared spectroscopy showed potential to discriminate species in different carbonization processes. Final temperature had a stronger influence on species distinction than the total processing time.

## Introduction

Charcoal is mainly used for energy purposes, but other important applications have been studied, such as improving soil properties for agriculture and absorbing pollutants, which are influenced by wood type, carbonization process and temperature, whereby the latter can increase sorption of organic compounds (Hale et al. 2016). A protocol for charcoal identification in Central Africa as a function of anatomical

---

✉ Silvana Nisgoski  
silvana.ufpr@gmail.com

Extended author information available on the last page of the article

structure preservation was described and evaluated by Hubau et al. (2012), showing its value for paleobotany and archeology.

Ranaivoson et al. (2017) described the use of 68 species for charcoal production in southwestern Madagascar and commented that in accordance with the country's forestry legislation, 21% of the species were protected or their use for charcoal making was prohibited, but local producers do not abandon the material because the product is preferred by consumers.

In Mozambique, a wide range of households and individuals produce charcoal for various reasons, such as to increase incomes (Jones et al. 2016) and for cooking. Its growing demand can lead to changes in the ecosystem service provision and woodland degradation while also significantly contributing to rural income and, possibly, poverty alleviation. As such, understanding of the charcoal production and trade has important implications for rural areas and for the sustainable development of woodland resources (Baumert et al. 2016). Two main charcoal supply chains from Mabalane to Maputo were observed by Baumert et al. (2016): (1) local operators produce charcoal on a small scale with household labor and selling to wholesalers; and (2) large-scale operators produce and sell large volumes of charcoal using migrant laborers, who sell their own production to wholesalers.

The impacts from charcoal production in tropical countries depend on forest management and natural regeneration, and since tree cutting is generally not selective, at site level, production leads to deforestation, while at landscape level, it leads to forest degradation (Chidumayo and Gumbo 2013). To transform the process into a sustainable activity, policy challenges must be taken into account. Afonso et al. (2015a), evaluating some Mozambican species, showed equivalent quality between charcoal produced from higher and lower commercial classes of wood, and indicated that species generally considered of low commercial value can be used efficiently to produce charcoal.

After the carbonization process, wood retains most of its anatomical characteristics, but its appearance is influenced by charring temperature and the proportion and distribution of vessels, parenchyma and fibers (Gasson et al. 2017). Thus, anatomical identification of charcoal can be done based on the intrinsic characteristics of species, and if a database is available, this process is facilitated (Gonçalves et al. 2012; Gonçalves and Scheel-Ybert 2016). Near-infrared (NIR) spectroscopy can also be a fast and nondestructive technique and shows potential for charcoal species identification and also differentiation of some processing characteristics (Davrieux et al. 2010; Monteiro et al. 2010; Muñiz et al. 2016; Nisgoski et al. 2018). The use of NIR portable equipment shows renewed interest by the scientific and industrial sector (Pasquini 2018).

In Mozambique, the use of wood classified as precious, first, second and third class (as a function of its commercial and scientific value, rarity, utility, resistance and quality) is not allowed for energy purposes (Ministério da Agricultura, 2002), but it is usual. Thus, to avoid illegal charcoal commerce, correct discrimination of the species is necessary, being important the use of techniques as anatomical and spectroscopic evaluations.

One disadvantage is that the practical applications of these techniques to charcoal species discrimination are dependent on a database. Based on this scenario,

**Table 1** List of species studied. (Source: Ministério da Agricultura (2002, 2007), Palgrave (2002))

Scientific name—Family	Commercial name	Commercial class <sup>a</sup>
<i>Androstachys johnsonii</i> Prain.—Picrodendraceae	Mecrusse	First
<i>Bobgunnia madagascariensis</i> (Desv.) J.H.Kirkbr. and Wiersema—Fabaceae	Pau ferro	First
<i>Sterculia quinqueloba</i> (Garcke) K. Schum.—Malvaceae	Metonha	Second

<sup>a</sup>Stated for wood commerce based on rarity, utility, resistance, quality, commercial and scientific value

**Table 2** Carbonization process parameters

Code	Final temperature (°C)	Total time	Reference
P1	400	40 min	Gonçalves et al. (2012)
P2	450	2 h	Nichols et al. (2000)
P3	450	4 h	Trugilho et al. (2005)
P4	450	6 h	Oliveira et al. (2010)

this study characterizes charcoal from three species not commercially authorized for energy purposes: *Androstachys johnsonii*, *Bobgunnia madagascariensis* and *Sterculia quinqueloba*, made by different carbonization processes. The impacts of the process parameters on wood anatomy and NIR spectroscopy were investigated to provide information to a database for charcoal identification and control.

## Materials and methods

### Material

Samples were collected randomly from Mozambican sawmills (Table 1) without identification of tree age or position in the trunk. The boards were divided into samples with the dimensions of 50 × 25 × 25 mm (tangential, radial and transversal sections). For each species, three samples were evaluated in each carbonization process. Wood and charcoal analyses were done on the same samples.

### Carbonization process

After wood anatomical evaluation, the samples were covered with aluminum foil and carbonized in an electric muffle furnace with four different programs (Table 2). The final temperature was chosen following the one traditionally employed by local people and also applied to charcoal characterization in scientific studies. After carbonization, samples remained in the furnace to cool, and the first step was spectroscopic evaluation.

## Near-infrared spectroscopy

NIR analyses were performed with a Bruker Tensor 37 spectrometer (Bruker Optics, Ettlingen, Germany) equipped with an integrating sphere and operating in reflectance mode with 64 scans, resolution of  $4\text{ cm}^{-1}$  and a spectral range of  $10,000\text{--}4000\text{ cm}^{-1}$ . In a room with a temperature of  $23 \pm 2\text{ }^\circ\text{C}$  and relative humidity of 60%, charcoal samples were placed on top of the integrating sphere and three spectra were obtained from each face (transversal, radial and tangential), resulting in a total of nine spectra for each physical sample, totaling 27 per species. Spectra from each surface were averaged, and analysis was done with three spectra per sample and nine spectra per species for each carbonization process.

The Unscrambler X chemometric program (version 10.1, from CAMO Software AS) was used to analyze the data. Exploratory modeling was done to verify the differences between the material by analyzing the score and loading graphs obtained by partial least square regression (PLS). Based on the loading graphs and a visual comparison of the mean spectra for each species and carbonization program, the wavenumber from  $4000\text{ to }5000\text{ cm}^{-1}$  was selected for posterior analysis. PLS with discriminant analysis (PLS-DA) was performed with mean centered data, applying the NIPALS algorithm and full cross-validation method with random nine segments to verify possible differences in charcoal as a function of the carbonization process or species. A linear discriminant analysis (LDA), based on the quadratic method assuming equal prior probabilities, was made with score data from PLS, and the confusion matrix was evaluated. Second derivative of Savitzky–Golay (polynomial order=2, smoothing point=21) was applied to raw data. Spectral analysis was based on ASTM E1655-05 (ASTM 2000).

## Anatomical characterization

Macroscopic analysis of wood and charcoal was done in a Zeiss Discovery v12 stereo microscope. Charcoal was broken by hand along the three structural planes of the wood, and the structure was analyzed. The qualitative anatomical features were described based on the procedures of the IAWA Committee (1989). The images from the surfaces of the three charcoal sections were taken by scanning electron microscopy (SEM) with a tabletop microscope (Hitachi TM-1000) along with direct observation of the sample material. The quantitative anatomical features were determined from the average of 25 measurements of the tangential diameter of the vessels, height and width of the rays and frequency of the vessels and rays.

Statistical analysis compared wood x charcoal and charcoal x charcoal with different carbonization programs. When data were normally distributed, mean values were compared by the Scott–Knott test at 5% probability, while for nonparametric data, analysis was done by the Kruskal–Wallis test, also at 5% of probability.

## Results and discussion

### Wood and charcoal anatomy

#### (a) *Androstachys johnsonii* (mecrusse)

The wood presented a few distinct growth rings, demarcated by thick-walled fibers (Fig. 1a); diffuse-porous, solitary vessel predominant and in radial multiples of 2 present, obstructed by gums; axial parenchyma diffuse; homogeneous rays with all cells procumbent, uniseriate, not storied (Fig. 1b); and fibers thick-walled. In charcoal, the qualitative characteristics remained in all carbonization processes, and it was possible to observe the distinction of growth rings (Fig. 1c, e, g, i) diffuse-porous, solitary vessel predominant; uniseriate rays, not storied (Fig. 1d, f, h, j). Some cracks were verified in rays at lower temperatures (Fig. 1D).

#### (b) *Sterculia quinqueloba* (metonha)

The wood presented a few distinct growth rings, demarcated by thick-walled fibers; diffuse-porous (Fig. 2a), solitary vessel predominant, radial multiples of 2–3 and cluster present, all vessels obstructed by tyloses; axial parenchyma in bands (Fig. 2a); heterogeneous rays, body ray cells procumbent with rows of square and/or upright marginal cells, multiseriate, not storied (Fig. 2b); fibers thick-walled. In charcoal, qualitative characteristics remained in all carbonization processes, and it was possible to observe obstruction in vessels (Fig. 2c, e, g, i), presence of splits in rays (Fig. 2f, g, h), multiseriate rays (Fig. 2d, f, h, j), the presence of crystals in parenchyma cells (Fig. 2d, e, i, j).

#### (c) *Bobgunnia madagascariensis* (pau ferro)

The wood presented growth rings which were indistinct or absent; diffuse-porous (Fig. 3a), vessels solitary and in radial multiples from 2 to 5, the presence of gums and other deposits; axial parenchyma in bands; homogeneous rays, all cells procumbent, radial multiples of 2–6 predominant, uniseriate rays present, all rays storied (Fig. 3B); fibers thick-walled. In charcoal, qualitative characteristics remained in all carbonization processes. It was possible to observe a better distinction of axial parenchyma (Fig. 3c, e, g, i) and multiseriate rays, not storied (Fig. 3d, f, h, j). In the carbonization process P1, some splits in the ray cells were observed (Fig. 3c).

Mean values of anatomical characteristics of the species are presented in Table 3.

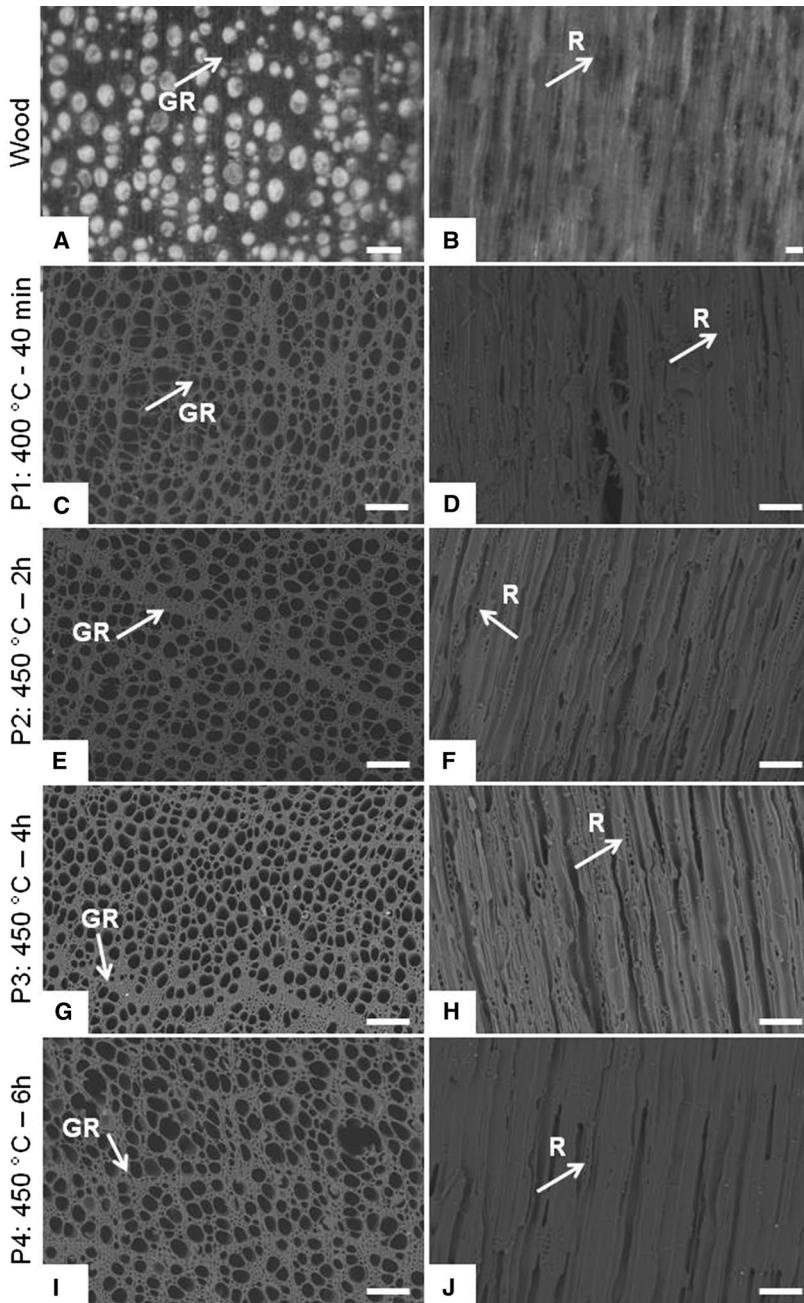


**Fig. 1** *Androstachys johnsonii* transverse (a, c, e, g, i) and tangential sections (b, d, f, h, j). Macroscopic images of wood (a, b) and SEM images of charcoal (c–j). Arrows indicate growth rings (GR) and uniseriate ray (R). Scale bar = 100  $\mu$ m

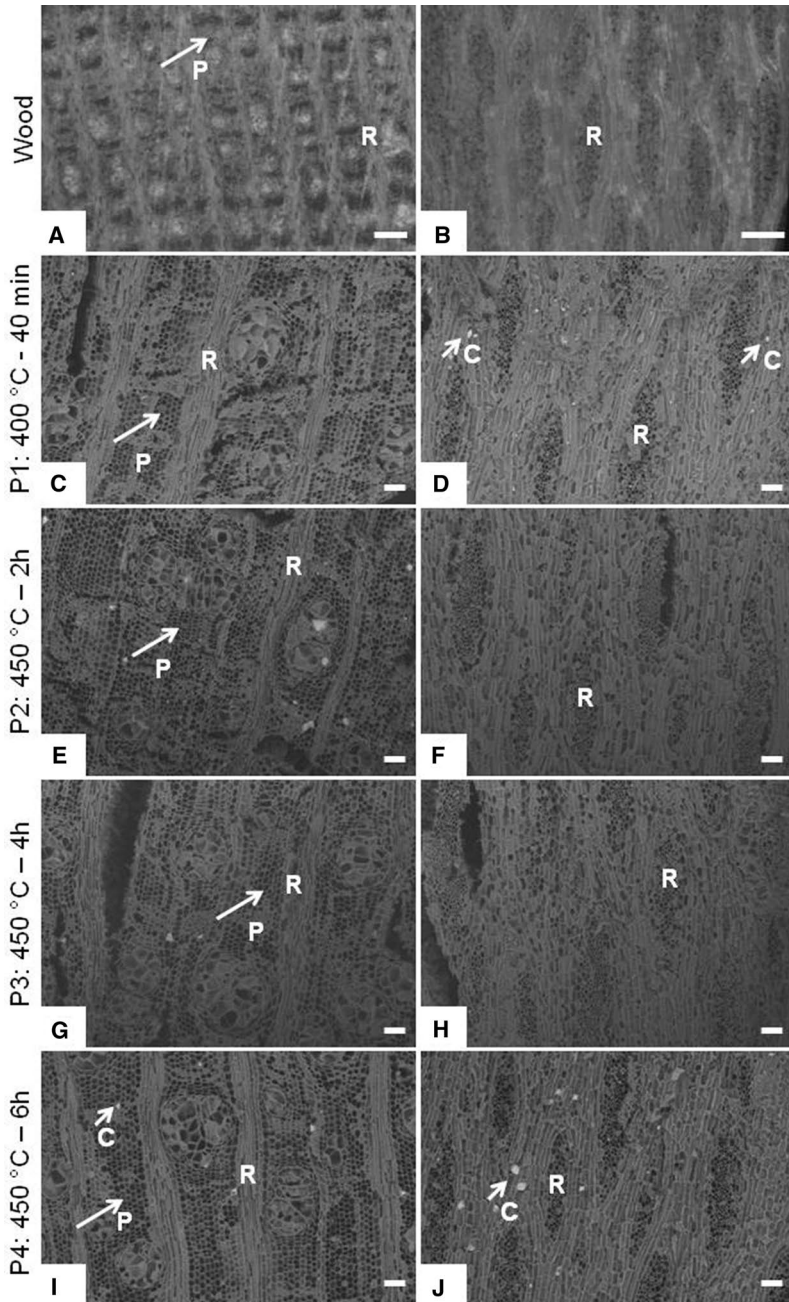


**Fig. 2** *Sterculia quinqueloba* transversal (a, c, e, g, i) and tangential sections (b, d, f, h, j). Macroscopic images of wood (a, b): scale bar=500  $\mu\text{m}$ . SEM images of charcoal (c–j): scale bar=100  $\mu\text{m}$ . Arrows indicate axial parenchyma (P) and crystal (C) in parenchyma cells; (R) multiseriate ray

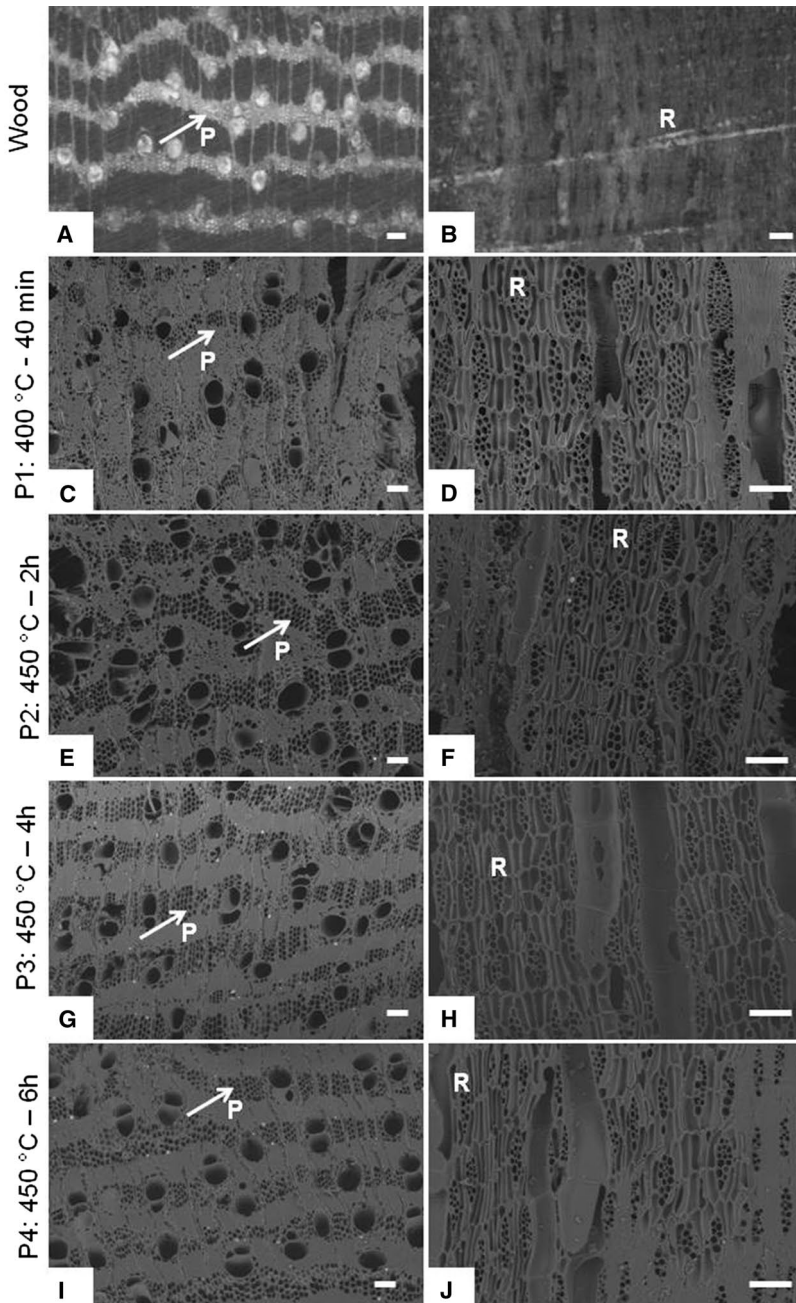


**Fig. 3** *Bobgunnia madagascariensis* transversal (a, c, e, g, i) and tangential sections (b, d, f, h, j). Macroscopic images of wood (a, b) and SEM images of charcoal (c–j). Arrow indicates axial parenchyma (P); (R) multiserial ray. Scale bar = 100  $\mu$ m



**Table 3** Mean values (and standard deviations) of wood and charcoal characteristics as a function of species and carbonization process

Species	Wood	Program Code			
		P1 400 °C 40 min	P2 450 °C 2 h	P3 450 °C 4 h	P4 450 °C 6 h
<b>Vessel diameter (µm)</b>					
<i>Androstachys johnsonii</i>	37.07 A (5.7)	33.02 Bb (5.0)	33.12 Bb (5.4)	35.96 Aa (5.4)	37.27 Aa (5.9)
<i>Sterculia quinqueloba</i>	259.84 A (43.9)	205.87 Ba (52.8)	174.52 Bb (31.5)	182.15 Bb (40.4)	196.04 Ba (36.7)
<i>Bobgunnia madagascariensis</i>	90.44 A (13.1)	100.44 Ab (22.3)	106.32 Ba (15.4)	95.55 Ab (11.1)	113.19 Ba (14.7)
<b>Vessels/mm<sup>2</sup></b>					
<i>Androstachys johnsonii</i>	203.55 A (20.3)	409.07 Bc (39.6)	481.33 Bb (40.3)	584.30 Ba (54.1)	474.43 Bb (65.8)
<i>Sterculia quinqueloba</i>	2.30 A (0.7)	2.37 Ab (1.2)	2.67 Aab (1.4)	2.63 Aab (1.1)	3.20 Ba (1.2)
<i>Bobgunnia madagascariensis</i>	11.73 A (2.5)	10.67 Ac (2.7)	20.77 Ba (4.5)	13.70 Bb (3.9)	14.47 Bb (4.7)
<b>Ray height (µm)</b>					
<i>Androstachys johnsonii</i>	113.81 A (23.5)	144.38 Ba (25.3)	108.26 Ab (25.6)	95.40 Bc (27.6)	114.77 Ab (32.5)
<i>Sterculia quinqueloba</i>	1322.46 A (467.1)	796.71 Ba (221.4)	532.71 Bc (155.41)	676.18 Bb (163.8)	826.88 Ba (198.1)
<i>Bobgunnia madagascariensis</i>	165.19 A (18.1)	191.52 Ba (27.2)	127.45 Bc (12.2)	135.26 Bc (15.0)	144.08 Bb (14.1)
<b>Ray width (µm)</b>					
<i>Androstachys johnsonii</i>	14.81 A (3.0)	27.78 Ba (6.7)	7.91 Bc (2.1)	10.53 Bb (2.8)	10.28 Bb (1.7)
<i>Sterculia quinqueloba</i>	234.27 A (55.4)	176.82 Ba (49.3)	110.25 Bc (2.87)	125.05 Bc (32.9)	152.64 Bb (17.7)
<i>Bobgunnia madagascariensis</i>	39.45 A (7.5)	53.40 Ba (11.8)	38.26 Ab (6.0)	30.27 Bc (6.8)	31.94 Bc (7.5)
<b>Ray/mm</b>					
<i>Androstachys johnsonii</i>	5.97 A (1.9)	6.20 Ab (1.6)	9.10 Ba (1.7)	9.70 Ba (2.1)	9.93 Ba (1.8)
<i>Sterculia quinqueloba</i>	1.53 A (0.5)	2.17 Bb (0.7)	2.87 Ba (0.7)	2.07 Bb (0.9)	2.73 Ba (0.6)
<i>Bobgunnia madagascariensis</i>	7.57 A (1.7)	6.37 Bb (1.3)	7.03 Ab (1.9)	8.70 Ba (1.8)	8.80 Ba (1.9)

Same small letters in a row indicate no difference between programs for each characteristic at 5% probability by the Scott–Knott or Kruskal–Wallis test. Same capital letters in a row indicate no difference between wood and charcoal for each characteristic at 5% probability by the Scott–Knott or Kruskal–Wallis test

## Tangential diameter of vessels

Evaluation of the changes in vessel diameter in *Androstachys johnsonii* samples after the carbonization process showed that charcoal produced with programs P1 and P2 underwent a decrease of 11% in wood dimension, and for P3 and P4, no statistical modifications occurred. When a comparison was made between carbonization programs, the results were similar at lower temperature and time of carbonization, with separation of two groups: P1 similar to P2 and P3 similar to P4.

In *Bobgunnia madagascariensis* samples, the carbonization process resulted in an increase in vessel diameter from wood to charcoal in all programs, but it only was statistically significant in P2 (increase of 18%) and P4 (increase of 25%). Comparing the carbonization processes, P1 was similar to P3, and P2 was similar to P4, the group with the highest values from P1/P3.

In *Sterculia quinqueloba* samples, a decrease in vessel diameter was observed after all carbonization processes, being higher in P2 (-33%) and P3 (-30%). In a comparison between charcoals produced with different programs, two groups were observed: P1/P4 and P2/P3.

In three of the species, structural modifications that occurred during transformation of wood in charcoal were different according to the carbonization programs. This was the result of the species' anatomical and chemical characteristics. Changes in tangential diameter of vessels are described in the literature as a result of material contraction and degradation of cell wall components (Poletto et al. 2012; Nisgoski et al. 2014; Pereira et al. 2016). Higher extractives content can be responsible for higher degradation of wood, and the cellulose crystallinity is related to the opposite behavior (Poletto et al. 2012).

Nisgoski et al. (2014), evaluating dimensional changes in *Ocotea porosa* with carbonization temperatures from 350 to 650 °C, stated that there was no significant influence of temperature on vessel diameter. Other literature sources have reported the influence of species on the decrease or increase in vessel dimension, and related the results to axial parenchyma type and fiber wall thickness. For example, Gonçalves et al. (2012) analyzed five Brazilian Cerrado species and found that vessel size was the wood feature most affected by carbonization; a significant reduction in tangential vessel diameter was observed in four out of five of the analyzed species. Muñiz et al. (2012) observed a significant reduction in vessel diameter in *Enterolobium schomburgkii* and no modifications in *Cedrelinga catenaeformis* carbonized at 450 °C and a heating rate of 1.66 °C min<sup>-1</sup>, and Stange et al. (2018) verified a reduction in vessel diameter of 21–33% in four Myrtaceae species under the same conditions. In addition, in *Eucalyptus* clones, Pereira et al. (2016) observed a mean reduction in vessel diameter of 18.6% with a similar carbonization process.

Another modification is related to the shape of cells and vessels from circular to angular after carbonization (e.g., Gonçalves et al. 2012). Gasson et al. (2017) described that in *Croton sonderianus*, the cells started losing their circular shape at 400 °C and became more angular and occasionally amorphous at 600 °C.

## Vessel frequency

In *Androstachys johnsonii* samples, the vessel frequency after carbonization increased with all programs by more than 100%, maybe because in charcoal, the vessels are more distinct. When the analysis between programs was done, no linear relation was observed. A higher value was verified in P3, similar values in P2 and P4 and a lower value in P1.

In *Bobgunnia madagascariensis*, the carbonization process with lower temperature and total time (P1) did not influence the vessel frequency, with the values being similar to those of wood. In P2, P3 and P4, an increase in vessel frequency was observed in charcoal, with higher values in P2 (+77%) and lower values in P3 (+17%). Regarding differences between carbonization processes, lower values were noted in P1 and higher values in P2, P3 and P4, which was not statistically different, showing more influence of temperature on the changes.

In *Sterculia quinqueloba*, the vessel frequency after the carbonization process increased by 39% in P4, while in the other programs, this feature was not statistically significant. Comparing programs, the highest vessel frequency was in P4 and the lowest in P1, while P2 was equal to P3 and similar to the others. These results show some interactions between temperature and total time.

Modifications in vessel frequency in the three species analyzed were different, possibly the result of intraspecific variability. The literature studies show that in general, carbonization results in contraction of cells, and in relation to vessels, causes an increase in their frequency (Pereira et al. 2016). In four Myrtaceae species, Stange et al. (2018) verified an increase in vessel frequency of 50–92% after carbonization with a final temperature of 450 °C and a heating rate of 1.66 °C min<sup>-1</sup>. Under the same conditions, Muñiz et al. (2016) observed an increase in vessel frequency in *Hymenolobium petraeum* and *Parkia pendula* and no changes in *Diploptropis purpurea*, *Vatairea guianensis* and *Vatairea paraensis*. The influence of species characteristics was also mentioned by Gonçalves and Scheel-Ybert (2016). Evaluating *Ocotea porosa* at four carbonization processes, Nisgoski et al. (2014) also showed that the differences in vessel frequency in the processes with the same final temperature of 450 °C was caused by the heating rate combined with the total time of carbonization. Gonçalves et al. (2012) found no significant change in vessel frequency, despite the significant reduction in tangential vessel diameter. This leads us to conclude that this feature is highly variable among species.

## Ray height

A different tendency was observed for ray height in *Androstachys johnsonii* after the carbonization process as a function of temperature and time of carbonization. With P1, an increase of 27% was observed, while a decrease of 16% was found in P3, and P2 and P4 had a similar ray height to wood. Among the programs, P1 showed the highest values and P3 the lowest.

In *Bobgunnia madagascariensis*, the ray height after the carbonization process presented variations in all programs. In P1, an increase of 16% was observed,

while in the other processes decreases of 23%, 18% and 13% occurred for P2, P3 and P4, respectively, related to the total process time. Among the programs, ray dimension was higher in P1, followed by P4, and was similar in P2 and P3, with the lowest values.

A decrease in ray height was verified in *Sterculia quinqueloba* samples after carbonization under all conditions. A reduction occurred in P2 (−60%), P3 (−49%), P1 (−40%) and P4 (−37%), with no linear relation as a function of temperature or total time. Regarding the programs, P1 was similar to P4 with the highest values, P2 presented the lowest dimension and P3 was intermediate. It is interesting that processing at the lowest temperature and total time (400 °C and 40 min) produced results similar to the highest temperature and total time (450 °C and 6 h).

Alterations in ray height are directly related to species characteristics, and no changes were observed based on temperature and time of carbonization in this study, corroborating the findings of Nisgoski et al. (2014) for *Ocotea porosa*. Muñiz et al. (2012) reported a different degradation of species with the same carbonization process as a function of fiber wall thickness, and Gonçalves et al. (2012) according to characteristics of ray cell composition. In a carbonization process with a final temperature of 450 °C and heating rate of 1.66 °C min<sup>−1</sup>, Muñiz et al. (2012) observed a reduction in ray height in *Enterolobium schomburgkii* and an increase in *Cedrelinga catenaeformis*. Nisgoski et al. (2015) reported a reduction in *Ficus citrifolia*, *Hieronyma laxiflora* and *Sapium glandulatum*, and no statistical changes in *Brosimum acutifolium*. Muñiz et al. (2016) verified a reduction in ray height for *Diploptropis purpurea* and no statistical changes in *Hymenolobium petraeum*, *Parkia pendula*, *Vatairea guianensis* and *Vatairea paraensis*, and Stange et al. (2018) observed increases from 10% to 24% in four Myrtaceae species.

## Ray width

In *Androstachys johnsonii* samples, a large increase in ray width occurred with P1 (+88%), and a decrease was observed for the other programs, from 47% with P2 to 29% with P3. Comparing only programs, P1 showed the highest value and P2 the lowest, while P3 and P4 were similar in intermediate position.

After carbonization, in *Bobgunnia madagascariensis* in P1 (400 °C and 40 min), an increase in ray width of 35% was verified, while with P2, the dimensions were not statistically different, and a decrease of 23% was verified in P3 and of 19% in P4. Evaluating ray width among the programs, P1 presented the highest dimensions, P2 was intermediate, and P3 and P4 were similar with lower values.

A decrease in ray width occurred after carbonization in all conditions for *Sterculia quinqueloba* samples, varying from 53% with P2 to 24% with P1, with a linear relation regarding time but not final temperature. Ray width was higher for P1, intermediate for P4, and the lowest in P2 and P3, which were similar.

A different dimensional variation is the result of anatomical characteristics of species, like the number of cells and ray width, whether the wood is homogeneous or heterogeneous, and also fiber wall thickness. Gonçalves et al. (2012) observed

a decrease in ray width in *Stryphnodendron polyphyllum*, *Croton grandiflora* and *Vochysia tucanorum*. Muñiz et al. (2012) verified a decrease in *Enterolobium schomburgkii* and an increase in *Cedrelinga catenaeformis*. Muñiz et al. (2016) reported a decrease in *Diplotropis purpurea* and *Parkia pendula*, and an increase in *Hymenolobium petraeum* and *Vatairea paraensis*, and no statistical changes in *Vatairea guianensis*. Stange et al. (2018) found an increase of 56% in *Myrcia retorta* and a decrease from 7% to 31% in other Myrtaceae species. Divergences can also be attributed to chemical changes in extractives which can expand and cause dimensional changes (Poletto et al. 2012; Pereira et al. 2016). On the other hand, Osterkamp et al. (2018), studying three species of *Araucaria*, found a positive correlation between ray width and carbonization temperature; the rays increased with an increase in temperature.

In a study on *Quercus variabilis*, Kim and Hanna (2006) reported that in multiseriate rays, some disintegration of cell walls occurred, and more ruptures were observed with increasing carbonization temperature. Nisgoski et al. (2014), comparing three final temperatures (350 °C, 450 °C and 650 °C) for carbonization of *Ocotea porosa*, noted that at 450 °C, the heating ramp had more influence in the presence of cracks and ruptures in rays. Afonso et al. (2015b) observed ruptures related to shrinkage in rays in Mozambican species carbonized at 450 °C for 1 h at a heating rate of 7.5 °C min<sup>-1</sup>. *Dalbergia melanoxylon* presented ruptures in a parallel direction and perpendicular to the rays, and *Pterocarpus angolensis* only had ruptures perpendicular to the rays. In other species (*Afzelia quanzensis*, *Amblygonocarpus andongensis*, *Guibourtia conjugata*, *Khaya nyasica* and *Swartzia madagascariensis*), only ruptures oriented in the direction of the rays were observed (Afonso et al. 2015b). Gonçalves et al. (2014) also verified ruptures in rays in some *Eucalyptus* species carbonized at 450 °C and a heating rate of 1.66 °C min<sup>-1</sup>, and under the same conditions, Gonçalves et al. (2018) reported ruptures in rays of some Cerrado species, while Osterkamp et al. (2018) reported the same for *Araucaria* spp.

## Ray frequency

For the *Androstachys johnsonii* samples, ray frequency in P1 with 400 °C and 40 min (least drastic conditions), there was no change in values. With 450 °C, an increase in ray frequency occurred with a linear relation to total time, varying from 52% for P2 (2 h) to 66% for P4 (6 h) and 62% for P3 (4 h). Comparing only the carbonization process, the ray frequency in P1 was lower, and similar values were observed for P2, P3 and P4.

In *Bobgunnia madagascariensis* samples, opposite alterations were observed for ray frequency in contrary conditions. In P1 (least drastic conditions, lower time and temperature), a reduction of 16% was verified and an increase of 16% occurred with P4 (most drastic conditions, highest time and temperature). With P2, no changes were observed, and with P3, an increase of 15% occurred, similar to P4. Evaluating only process conditions, P1 was similar to P2, with lower values and P3 was similar to P4 with higher values, indicating more influence of heating rate and total time.

After carbonization of *Sterculia quinqueloba* wood in all conditions, an increase in ray frequency was observed. Changes varied from 88% for P2 to 35% for P3, with

no direct relation to temperature or total time of carbonization. Analyzing only the carbonization processes, in ray frequency, two groups occurred: charcoal samples produced with P1/P3 and P2/P4 were similar.

Changes in ray frequency are also related to fiber cell wall thickness and axial parenchyma distribution, possibly specific or intraspecific, and ecological trends can be involved (Ávila et al. 2017). The results obtained in this study are in accordance with those of Nisgoski et al. (2014), who found that the different final carbonization temperatures did not significantly influence the ray frequency. In all situations, an increase was only observed from wood to charcoal, but not between carbonization programs.

In a carbonization process at 450 °C and heating rate of 1.66 °C min<sup>-1</sup>, increases in ray frequency were observed in four Myrtaceae species (Stange et al. 2018), in *Diplotropis purpurea*, *Hymenolobium petraeum* and *Vatairea guianensis* (Muñiz et al. 2016), and in *Ficus citrifolia*, *Hieronyma laxiflora* and *Sapium glandulatum* (Nisgoski et al. 2015). On the other hand, reduction in ray frequency was found in *Brosimum acutifolium* (Nisgoski et al. 2015), while no statistical changes occurred in *Parkia pendula* and *Vatairea paraensis* (Muñiz et al. 2016).

### Near-infrared spectroscopy

Raw spectra showed similarity between samples (Fig. 4a), and the second derivative was applied as pretreatment (Fig. 4b) to eliminate the influence of baseline and some noise. Mean second-derivative NIR spectra by species and program in the region from 4000 to 5000 cm<sup>-1</sup> showed the most contrast between carbonization programs (Fig. 4c), principally from program P1, with lower temperature and total time. The bands depicted in the figure are related to cell wall components, and also specifically at 4686 cm<sup>-1</sup> to extractives and at 4235 cm<sup>-1</sup> to cellulose content (Schwaninger et al. 2011). The near spectral signature in charcoal varies as a function of final temperature; higher temperatures result in lower absorbance bands (Costa et al. 2018), and differences in degradation of cell wall components at different times and temperatures are related to species characteristics (Rutherford et al. 2005; Poletto et al. 2012).

Pretreatment with second derivative in charcoal NIR spectra has also been applied in other studies on charcoal species discrimination (Muñiz et al. 2016; Nisgoski et al. 2018). In particular, Sandak et al. (2016) reported a decrease in absorbance values with increasing temperatures, and that not all bands changed at the same rate and intensity, so the chemical information after second-derivative application is still preserved and the pretreatment effectively removes the scatter and some noise. Program 1 (P1) had the lowest temperature and total time, resulting in the start of cell wall degradation, while the other programs, with 450 °C and total time varying from 2 to 6 h, caused more deterioration of chemical compounds in the cell walls. The rate of changes in each species has been related to wood density (Hidayat et al. 2017), extractive content (Pereira et al. 2016) and cellulose crystallinity (Poletto et al. 2012). These factors are dependent on wood anatomy, type and distribution of parenchyma cells and fiber cell wall thickness

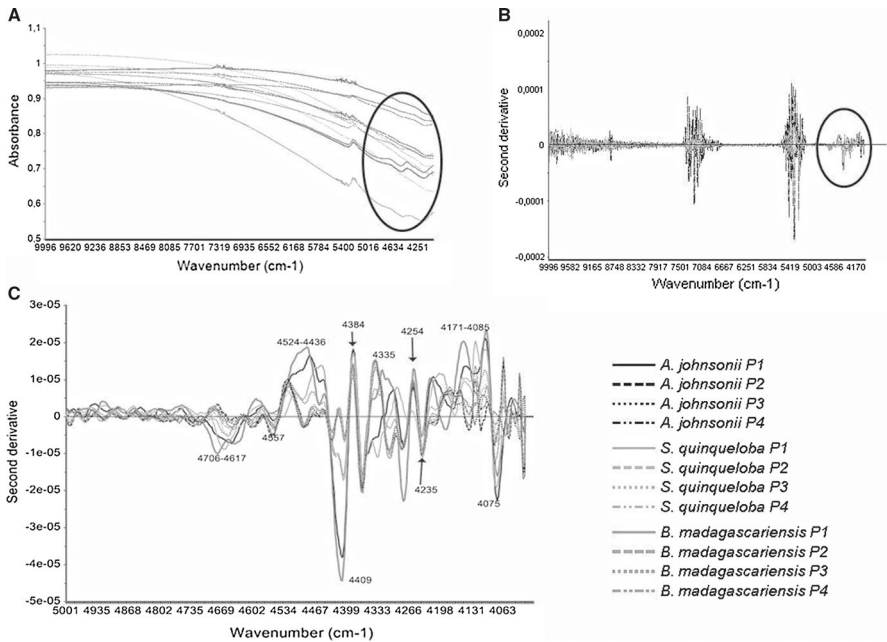


**Fig. 4** Mean NIR spectra from all the species in four carbonization processes: raw data (a) and second derivative (b) in wavenumbers from 4000 to 10000  $\text{cm}^{-1}$ ; second derivative in the region 4000–5000  $\text{cm}^{-1}$  (c)

and vessel diameter, as recounted by Gasson et al. (2017) for *Croton sonderianus* in comparison with other species described in the literature.

The influence of wood anatomy on spectra is corroborated by the present results, where *Sterculia quinqueloba* (Fig. 4—gray line), with the highest vessel diameter and axial parenchyma in bands, showed different NIR absorbance values compared to *Androstachys johnsonii* (Fig. 4—black line), with the lowest vessel diameter and diffuse axial parenchyma values.

It was not verified the influence of anatomical section where spectra were obtained in this study (graphic not shown). This fact was also commented by Muñiz et al. (2016) and Nisgoski et al. (2018), which is important for the practical use in industry or commerce inspections.

The score graphic (Fig. 5) from partial least squares regression with discriminant analysis (PLS-DA) done with second-derivative spectra in the region from 4000 to 5000  $\text{cm}^{-1}$  revealed the separation of samples carbonized with lower intensity (P1), with lower temperature and total time, with the other programs (P2, P3, P4) causing minor degradation of species, with some similarity to three samples of *Bobgunia madagascariensis* carbonized by P3, indicating final temperature had the most influence.

The graphic analysis based on species discrimination in each program allowed for the following observations: (1) in P1 (400 °C and 40 min), all species could be identified, with some similarity of *Androstachys johnsonii* and *Sterculia quinqueloba*

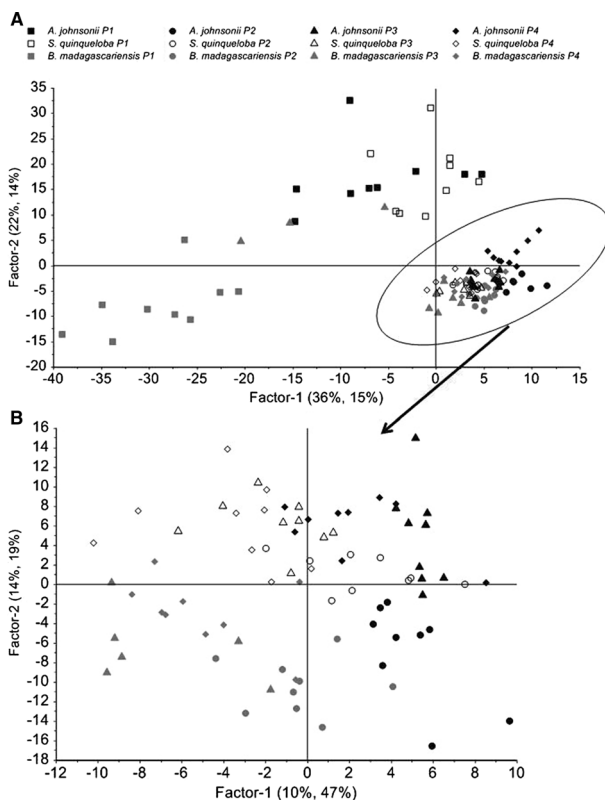


**Fig. 5** Score graph from PLS-DA with second-derivative NIR spectra with all carbonization programs (a) and with the final temperature of 450 °C only (b) in the region 4000–5000  $\text{cm}^{-1}$

samples; (2) in P2 (450 °C and 2 h), also all species could be identified even so with some “nearby” samples of *Androstachys johnsonii* and *Bobgunnia madagascariensis*; in P3 (450 °C and 4 h), samples from all species are distant and can be discriminated; and in P4 (450 °C and 6 h), samples from *Bobgunnia madagascariensis* are more isolated, and samples of *Androstachys johnsonii* and *Sterculia quinqueloba* showed some proximity. These data are the result of different changes in anatomical and chemical characteristics of each species in the same process, which has also been reported by other authors, like Gasson et al. (2017), Gonçalves and Scheel-Ybert (2016) and Muñoz et al. (2013).

The observations were confirmed by a confusion matrix based on PLS scores analysis from all carbonization programs (Table 4).

The factor 1 loading graph (Fig. 6) shows the wavenumber regions related to carbonization program distinction, as 4675, 4630, 4422–4395, 4270  $\text{cm}^{-1}$ , attributed to cell wall composition (Schwanninger et al. 2011). Muñoz et al. (2013) verified that the bands at 4253  $\text{cm}^{-1}$  and 4740  $\text{cm}^{-1}$ , related to lignin groups, were the regions responsible for the discrimination of charcoal from *Eucalyptus alba*,



**Table 4** Confusion matrix based on PLS-DA scores analysis from samples of all carbonization programs

Species/programs	P1			P2			P3			P4		
	<i>A. johnsonii</i>	<i>S. quinque-loba</i>	<i>B. madagascariensis</i>	<i>A. johnsonii</i>	<i>S. quinque-loba</i>	<i>B. madagascariensis</i>	<i>A. johnsonii</i>	<i>S. quinque-loba</i>	<i>B. madagascariensis</i>	<i>A. johnsonii</i>	<i>S. quinque-loba</i>	<i>B. madagascariensis</i>
<i>A. johnsonii</i> –P1	5	1	0	0	0	0	0	0	0	0	0	0
<i>S. quinque-loba</i> –P1	3	8	0	0	0	0	0	0	1	0	0	0
<i>B. madagascariensis</i> –P1	0	0	9	0	0	0	0	0	2	0	0	0
<i>A. johnsonii</i> –P2	0	0	0	9	0	1	0	0	0	0	0	0
<i>S. quinque-loba</i> –P2	0	0	0	0	8	0	1	1	0	2	1	1
<i>B. madagascariensis</i> –P2	0	0	0	0	0	7	0	0	2	0	1	1
<i>A. johnsonii</i> –P3	0	0	0	0	0	0	8	0	0	1	0	0
<i>S. quinque-loba</i> –P3	0	0	0	0	1	0	0	6	0	3	4	0
<i>B. madagascariensis</i> –P3	1	0	0	0	0	1	0	0	4	0	0	0
<i>A. johnsonii</i> –P4	0	0	0	0	0	0	0	1	0	3	0	0
<i>S. quinque-loba</i> –P4	0	0	0	0	0	0	0	1	0	0	2	0
<i>B. madagascariensis</i> –P4	0	0	0	0	0	0	0	0	0	0	1	7

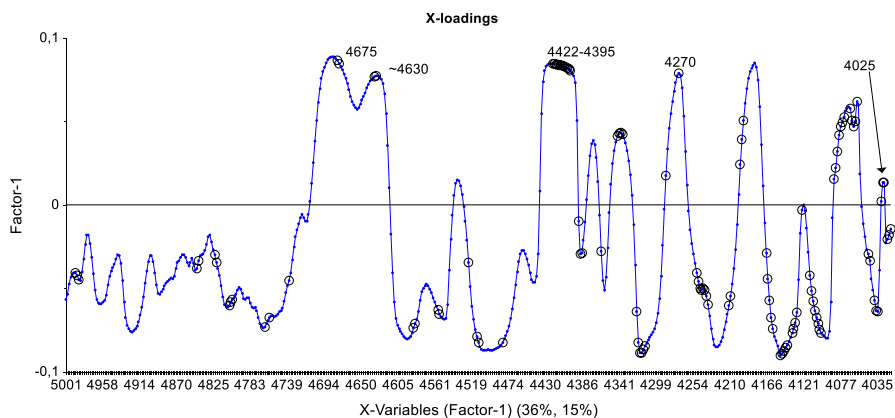


**Fig. 6** X-Loading graph of factor 1 based on second-derivative NIR spectra in the region 4000–5000  $\text{cm}^{-1}$

*Mimosa scabrella*, *Tabebuia capitata* and *Hymenaea aurea*, and also commented that the different degradation degrees were the result of anatomical and chemical characteristic of species. Muñiz et al. (2016) described the regions 4000–5000 and 5500–6200  $\text{cm}^{-1}$  as the best ones for distinguishing charcoal from “angelim” species. Nisgoski et al. (2018) verified that for charcoal, bands in the regions from 4000 to 5000  $\text{cm}^{-1}$  were better for the discrimination of six Caatinga species, supporting the influence of individual species.

Comparing industrial and laboratory charcoal, Monteiro et al. (2010) found that NIR spectroscopy, using data after first derivative treatment, was able to discriminate charcoal produced in an industrial process from that produced under laboratory conditions, but not to distinguish whether it was from native or exotic wood. The same finding was reported by Ramalho et al. (2017) in charcoal from *Cedrela* sp., *Aspidosperma* sp., *Jacaranda* sp., *Apuleia* sp. and eucalyptus clones pyrolyzed under controlled laboratory conditions at final temperatures of 300, 500 and 700  $^{\circ}\text{C}$ , which did not allow differentiating charcoal if all samples were analyzed at the same time. However, the separation of charcoal from native and planted trees was achieved when the samples were analyzed separately according to the final temperature. On the other hand, no clear separation in PCA analysis of charcoal specimens as a function of the final carbonization temperature, especially for material pyrolyzed at 400, 500 and 600  $^{\circ}\text{C}$ , was noted by Costa et al. (2018) for eucalypt. Davrieux et al. (2010) detailed the distinction of *Tabebuia serratifolia* from *Eucalyptus grandis* carbonized at 400  $^{\circ}\text{C}$  and a heating rate of approximately 3.81  $^{\circ}\text{C min}^{-1}$ .

In species identification, some studies have shown that in thermal degradation, the temperature ranges responsible for correct classifications are the result of single component decomposition, mainly hemicelluloses (Tarrío-Saavedra et al. 2011). The thermal decomposition of wood depends on the mass ratio of its main components, hemicellulose, cellulose and lignin. The temperature ranges of hemicellulose and cellulose decomposition are about 220–315  $^{\circ}\text{C}$  and 315–400  $^{\circ}\text{C}$ , and thermal decomposition of lignin occurs in a wide temperature range from 180  $^{\circ}\text{C}$  to 900  $^{\circ}\text{C}$ . The thermal

degradation process can be affected by operating parameters such as temperature, pressure, heating rate or by the properties of the biomass used, such as shape and size of particles, composition and moisture. The size and shape of the particles influence the heat transfer into the particles and mass transfer from the particles (Gasparovic et al. 2012). In nine wood samples pyrolyzed at temperatures from 30 °C until 1200 °C, Smith et al. (2012) observed that between 30 and 250 °C, no large changes occurred in the nanostructure of cellulose microfibrils, while between 250 and 315 °C, the structure of cellulose fibrils completely degraded, and until 1200 °C, nanometer-sized inhomogeneities in the material appeared.

The evolution of charcoal production with time and temperature treatment, on a molar basis, is evaluated by the hydrogen/carbon and oxygen/carbon atomic ratios. An increase in percentage of aromatic carbon can be the result of its formation in the charring process or by the removal of aliphatic components during charring. At 250 °C and 300 °C, an increase in total mass of aromatic carbon in pine and poplar wood was verified by Rutherford et al. (2005), and at 350 °C and above, a more rapid decrease in aromatic carbon after the first hour of heating was observed. The wood or wood components do not contain measurable porosity, but develop this porosity during charring (Rutherford et al. 2005). At the same carbonization temperature, the char yield was higher in wood with greater initial density, as reported by Hidayat et al. (2017), in a study with mangium, mindi, gmelina and albizia. In addition, another study commented that fiber dimensions and principally cell wall fraction influence the charcoal density (Pereira et al. 2016).

In this study, the three evaluated species have medium-to-high density and present thick-walled fibers. The differences are in vessel diameter and type of axial parenchyma, which can explain some divergence in the results. Since near-infrared spectra are based on cell components, charcoal produced with diverse programs presents changes in absorbance/reflectance at some wavenumbers related to cellulose, hemicelluloses, lignin and extractives, as a function of degradation according to temperature. The final temperature showed more influence on grouping samples in relation to total process time, but all species could be individually identified, enabling application of this technique to forest control.

## Conclusion

In the three species analyzed, changes in anatomical characteristics after carbonization were different, and groups were formed regarding charcoal programs, as a result of anatomical and chemical characteristics. In vessel and ray dimensions and frequency, no linear relation to total time or final carbonization temperature was observed, although there were some interactions between species and program conditions.

In the near-infrared spectra, the region from 4000 to 5000  $\text{cm}^{-1}$  showed more distinction between wood and charcoal. There was a separation of samples carbonized with lower intensity (400 °C and 40 min), denoting minor chemical degradation of species, from samples submitted to other programs with a final temperature of 450 °C and total time between 2 and 6 h. Near-infrared spectrometry

showed potential to discriminate species in different carbonization process. The final temperature had a stronger influence on charcoal species distinction than the total process time.

**Acknowledgements** We would like to thank the Ford Foundation, *Conselho Nacional de Desenvolvimento - CNPQ* Brazil (PQ 303374/2016-0), and *Coordenação de Aperfeiçoamento de Pessoal de Nível Superior - CAPES* Brazil (Financial Code 001).

## References

- Afonso CMI, Gonçalves TAP, Muñiz GIB, Matos JLM, Nisgoski S (2015a) Mozambique's charcoals—energetic properties of nine native species. *Eur J Wood Prod* 73:131–133
- Afonso CMI, Gonçalves TAP, Muñiz GIB, Matos JLM, Nisgoski S (2015b) Mozambique's charcoals: anatomy of nine native species. *Bosque* 36:105–112
- ASTM (2000) ASTM E1655—Standard practices for infrared multivariate, quantitative analysis. Vol.03.06. American Society for Testing and Materials, West Conshohocken, Pennsylvania, USA
- Ávila A, Giongo C, Scheel-Ybert R (2017) Charcoal anatomy of 10 native species of Rio Grande do Sul coastal plain (Brazil)—a support for archaeological and paleoecological research. *Cadernos do LEPAARQ (UFPEL)* 14:482–511. (In Portuguese)
- Baumert S, Luz AC, Fisher J, Vollmer F, Ryan CM, Patenaude G, Zorrilla-Miras P, Artur L, Nhantumbo I, Macqueen D (2016) Charcoal supply chains from Mabalane to Maputo: who benefits? *Energy Sustain Dev* 33:129–138
- Chidumayo EN, Gumbo DJ (2013) The environmental impacts of charcoal production in tropical ecosystems of the world: a synthesis. *Energy Sustain Dev* 17:86–94
- Committee IAWA (1989) IAWA list of microscopic features for hardwood identification. *IAWA Bull* 10:219–332
- Costa LR, Trugilho PF, Hein PRG (2018) Evaluation and classification of eucalypt charcoal quality by near infrared spectroscopy. *Biomass Bioenerg* 112:85–92
- Davrieux F, Rousset PLA, Pastore TCM, Macedo LA, Quirino WF (2010) Discrimination of native wood charcoal by infrared spectroscopy. *Quim Nova* 33:1093–1097
- Gasparovic L, Labovsky J, Markos J, Jelemensky L (2012) Calculation of kinetic parameters of the thermal decomposition of wood by distributed activation energy model (DAEM). *Chem Biochem Eng Q* 26:45–53
- Gasson P, Cartwright C, Dias Leme CL (2017) Anatomical changes to the wood of *Croton sonderianus* (Euphorbiaceae) when charred at different temperatures. *IAWA J* 38:117–123
- Gonçalves TAP, Scheel-Ybert R (2016) Charcoal anatomy of Brazilian species. I. Anacardiaceae. *Anais Acad Bras de Cien* 88:1711–1725
- Gonçalves TAP, Marcati CR, Scheel-Ybert R (2012) The effect of carbonization on wood structure of *Dalbergia violaceae*, *Stryphnodendron polyphyllum*, *Tapirira guianensis*, *Vochysia tucanorum* and *Pouteria torta* from the Brazilian Cerrado. *IAWA J* 33:73–90
- Gonçalves TAP, Ballarin AW, Nisgoski S, Muñiz GIB (2014) A contribution to the identification of charcoal origin in Brazil I - Anatomical characterization of *Corymbia* and *Eucalyptus*. *Maderas. Ciencia y Tecnol* 16:323–336
- Gonçalves TAP, Oliveira JS, Nisgoski S, Marcati CR, Ballarin AW, Muñiz GIB (2018) A contribution to the identification of charcoal origin in Brazil III: microscopic identification of 10 Cerrado species. *Aust J Bot* 66:255–264
- Hale SE, Arp HPH, Kupryianchuk D, Cornelissen G (2016) A synthesis of parameters related to the binding of neutral organic compounds to charcoal. *Chemosphere* 144:65–74
- Hidayat W, Qi Y, Jang JH, Febrianto F, Lee SH, Chae HM, Kondo T, Kim NH (2017) Carbonization characteristics of juvenile woods from some tropical trees planted in Indonesia. *J Fac Agr Kyushu Univ* 62:145–152

- Hubau W, den Bulcke JV, Kitin P, Mees F, Acker JV, Beeckman H (2012) Charcoal identification in species-rich biomes: a protocol for Central Africa optimized for the Mayumbe Forest. *Rev Palaeobot Palynol* 171:164–178
- Jones D, Ryan CM, Fisher J (2016) Charcoal as a diversification strategy: the flexible role of charcoal production in the livelihoods of smallholders in central Mozambique. *Energy Sustain Dev* 32:14–21
- Kim NH, Hanna RB (2006) Morphological characteristics *Quercus variabilis* charcoal prepared at different temperatures. *Wood Sci Technol* 40:392–401
- Ministério da Agricultura (2002) Regulamento da Lei de Fauna e Florestas Bravias. Decreto 12/2002. (Regulation of the Forest and Wildlife Law. Decree 12/2002). Maputo, Mozambique 2002. pp.1–45
- Ministério da Agricultura (2007) Diploma Ministerial n°.8/2007, 24 de janeiro de 2007.(Ministerial Diploma 8/2007, January 24, 2007)
- Monteiro TC, Silva RV, Lima JT, Hein PRG, Napoli A (2010) Use of near infrared spectroscopy to distinguish carbonization processes and charcoal sources. *Cerne* 16:381–390
- Muñiz GIB, Nisgoski S, França RF, Schardosin FZ (2012) Comparative anatomy of wood and charcoal of *Cedrelinga catenaeformis* Ducke and *Enterolobium schomburgkii* Benth. for identification purposes. *Sci For* 40:291–297
- Muñiz GIB, Carneiro ME, Nisgoski S, Ramirez MGL, Magalhães WLE (2013) SEM and NIR characterization of four charcoal species. *Wood Sci Technol* 47:815–823
- Muñiz GIB, Carneiro ME, Batista FRR, Schardosin FZS, Nisgoski S (2016) Wood and charcoal identification of five species from the miscellaneous group known in Brazil as “angelim” by near-ir and wood anatomy. *Maderas. Ciencia y Tecnol* 18:505–522
- Nichols GJ, Cripps JA, Collinson ME, Scott AC (2000) Experiments in waterlogging and sedimentology of charcoal: results and implications. *Palaeogeogr Palaeoclimatol Palaeoecol* 164:43–56
- Nisgoski S, Muñiz GIB, Batista FRR, Mülleken RE (2014) Influence of carbonization temperature on the anatomical characteristics of *Ocotea porosa* (Nees & Mart. Ex Nees) L. Barroso. *Wood Sci Technol* 48:301–309
- Nisgoski S, Muñiz GIB, Morrone SR, Schardosin FZ, França RF (2015) NIR and anatomy of wood and charcoal from Moraceae and Euphorbiaceae species. *Ciência da Madeira* 6:183–190
- Nisgoski S, Batista FRR, Naide TL, Laube NCC, Leão ACR, Muñiz GIB (2018) Discrimination of wood and charcoal from six caatinga species by near-infrared spectroscopy. *Maderas. Ciencia y Tecnol* 20:199–210
- Oliveira AC, Carneiro ACO, Vital BR, Almeida W, Pereira BLC, Cardoso MT (2010) Quality parameters of *Eucalyptus pellita* F. Muell. wood and charcoal. *Sci For* 38:431–439
- Osterkamp IC, de Lara DM, Gonçalves TAP, Kauffmann M, Périco E, Stülp S, Machado NTG, Uhl D, Jasper A (2018) Changes of wood anatomical characters of selected species of Araucaria during artificial charring: implications for paleontology. *Acta Bot Bras* 32(2):198–211
- Palgrave KC (2002) *Trees of Southern Africa*, 3rd ed. Struik Nature, South Africa 2002
- Pasquini C (2018) Near infrared spectroscopy: a mature analytical technique with new perspectives—a review. *Anal Chim Acta* 1026:8–36
- Pereira BLC, Carvalho AMML, Oliveira ACO, Santos LCS, Carneiro ACO, Magalhães MA (2016) Effect of wood carbonization in the anatomical structure and density of charcoal from *Eucalyptus*. *Ciência Florestal* 26:545–557 (In Portuguese)
- Poletto M, Zattera AJ, Santana RMC (2012) Thermal decomposition of wood: kinetics and degradation mechanisms. *Biores Technol* 126:7–12
- Ramalho FMG, Hein PRG, Andrade JM, Napoli A (2017) Potential of near-infrared spectroscopy for distinguishing charcoal produced from planted and native wood for energy purpose. *Energy Fuels* 31:1593–1599
- Ranaivoson T, Rakouth B, Buerkert A, Brinkmann K (2017) Wood biomass availability for smallholder charcoal production in dry forest and savannah ecosystems of south-western Madagascar. *J Arid Environ* 146:86–94
- Rutherford DW, Wershaw RL, Cox LG (2005) Changes in composition and porosity occurring during the thermal degradation of wood and wood components. Scientific Investigations Report 2004-5292. U.S. Geological Survey, Reston, Virginia, p 88
- Sandak J, Sandak A, Allegretti O (2016) Chemical changes to woody polymers due to high-temperature thermal treatment assessed with near infrared spectroscopy. *J Near Infrared Spectrosc* 24:555–562
- Schwanninger M, Rodrigues JC, Fackler K (2011) A review of band assignments in near infrared spectra of wood and wood components. *J Near Infrared Spectrosc* 19:287–308

- Smith AJ, MacDonald MJ, Ellis LD, Obrovac MN, Dahn JR (2012) A small angle X-ray scattering and electrochemical study of the decomposition of wood during pyrolysis. *Carbon* 50:3717–3723
- Stange R, Vieira HC, Rios PD, Nisgoski S (2018) Wood and charcoal anatomy of four Myrtaceae species. *Cerne* 24:190–200
- Tarrío-Saavedra J, Naya S, Francisco-Fernández M, López-Beceiro J, Artiaga R (2011) Functional nonparametric classification of wood species from thermal data. *J Thermochem Analytic Cal* 104:87–100
- Trugilho PF, Silva JRM, Mori FA, Lima JT, Mendes LM, Mendes LFB (2005) Yield and charcoal characteristics in relation of radial sampling position in *Eucalyptus* clones. *Cerne* 11:178–186

**Publisher's Note** Springer Nature remains neutral with regard to jurisdictional claims in published maps and institutional affiliations.

## Affiliations

**Silvana Nisgoski<sup>1</sup>**  · **Helena Cristina Vieira<sup>2</sup>** · **Thaís Alves Pereira Gonçalves<sup>3</sup>** · **Claudio Manuel Afonso<sup>4</sup>** · **Graciela Inés Bolzon de Muñiz<sup>1</sup>**

Helena Cristina Vieira  
lenacristin@gmail.com

Thaís Alves Pereira Gonçalves  
th\_goncalves@yahoo.com.br

Claudio Manuel Afonso  
claudioafonso@live.com

- <sup>1</sup> Department of Forest Engineering and Technology, Federal University of Parana, Av. Prof. Lothário Meissner, 632, Jardim Botânico, Curitiba, Paraná 80.210-170, Brazil
- <sup>2</sup> Post-Graduate Program in Forest Engineering, Federal University of Parana, Av. Prof. Lothário Meissner, 632, Jardim Botânico, Curitiba, Paraná 80.210-170, Brazil
- <sup>3</sup> Department of Forest Engineering, University From Santa Catarina State, Av. Luis de Camões, 2090, Bairro Conta Dinheiro, Lages, Santa Catarina 88520-000, Brazil
- <sup>4</sup> Ministry of Agriculture, National Directorate of Land and Forestry, Av. Josina Machel, 537, Maputo, Mozambique